

Monte Carlo Modeling of the Light Transport in Polymer Light-Emitting Devices on Plastic Substrates

Shu-jeen Lee, Aldo Badano, and Jerzy Kanicki, *Senior Member, IEEE*

Abstract—A Monte Carlo method for modeling the light transport phenomena in organic polymer light-emitting devices (PLEDs) has been reported previously (Badano and Kanicki, 2001). The advantage of this simulation method is its ability to model bulk absorption, thin-film coatings, and uneven or irregular surfaces by tracking the photon polarization in realistic device structures. We have applied this method to analyze the PLEDs spectral outputs and out-coupling efficiencies. We have established that the calculated out-coupling efficiencies are approximately the same ($\eta_{\text{coup}} \sim 0.2$) for the red and green PLEDs. Using a description of uneven surfaces with Fresnel analysis, we showed that the nonsmooth interfaces (as modeled by the algorithm for uneven surfaces) between light-emitting polymer and hole transporting layer increase the probabilities of out-coupling and wave-guiding of the internally generated light. In this paper, we use this method to calculate the angular distribution of the PLED light-emission. We found that the Monte Carlo simulated PLED light-emission angular distribution shows better agreement with the experimental data than previously used models relying on standard refraction theory at one interface [2].

Index Terms—Monte Carlo simulation, out-coupling efficiency, plastic substrate, polymer light-emitting devices.

I. INTRODUCTION

IN GENERAL, it is accepted that the external quantum efficiency of the organic polymer light-emitting devices (PLEDs) is limited by several major losses: charge injection at the contacts (anode and cathode), charge transport within the organic materials, electron and hole radiative recombination, photoluminescent efficiency, and light out-coupling efficiency [3]. Using a standard refraction theory, it was estimated that the photon out-coupling efficiency is about 1/5 of the total internally generated photons [2]. Several methods for improving the light out-coupling efficiency have been used to overcome this limitation set by the light escape cone of the substrate. These methods include introduction of textured surfaces or interfaces [4], [5], usage of ordered microlens arrays or microsphere media [6], [7], usage of reflecting surfaces or distributed Bragg

reflectors [8], [9], and usage of a thin silica aerogel layer [10]. Several models have also been proposed for modeling optical transport in organic light-emitting devices, such as the half-space optical model [11], one-dimensional ray-tracing [5], and quantum mechanical microcavity model [12], [13], [26]. We have used a Monte Carlo approach to analyze the PLED light out-coupling efficiency [1]. This method has the flexibility for modeling events such as absorption, wave-guiding, scattering, out-coupling, and trapping in the light-emitting devices. The advantage of the Monte Carlo simulation method is that it takes into account the details of device geometry. The Monte Carlo simulation includes the angular and spectral distributions of the emitted photons, the point-spread function, the specular and diffuse reflection coefficients, and a summary of scattering events statistics.

In this paper, we describe the results of Monte Carlo simulation used to investigate the factors contributing to PLED angular light-emission pattern. Also, the effect of the nonsmooth interfaces on the PLED light out-coupling efficiency is simulated. The simulation results are compared with the PLED experimental results.

II. METHODS

A. Optical Modeling

In this paper, we used a Monte Carlo method for the simulation of light transport processes in PLEDs [1], [14], [24]. This code, originally developed to study light transport in radiation detectors has been improved in the physics description and in its ability to model light-emissive structures typical of flat-panel display devices. The current version of the code, DETECT-II, is being used to investigate light transport problems in detectors [16], cathode-luminescent display devices [17], and thin-film light-emissive devices. The Monte Carlo method makes use of the generation of photons with random direction according to a distribution function describing the nature of the light-emission. In this analysis, the light source within the organic polymer layer is considered isotropic from a single point situated in the center of the device, Fig. 1. We assumed the light source being described by the photoluminescence (PL) spectra of the light-emitting materials [24]. The photon histories are then followed through a sequence of interactions that includes absorption and Fresnel refraction. At the optical boundaries, an analysis is performed depending on the surface type and material properties using Fresnel's equations and considering the polarization of the incoming photon [1]. When the film thickness is comparable with the photon wavelength, we use modified Fresnel coefficients to describe the optically thin-film effect. The reflection

Manuscript received June 9, 2003; revised October 20, 2003. This work was supported by the National Institutes of Health (NIH) grant.

S. Lee is with the Macromolecular Science and Engineering and the Solid-State Electronics Laboratory, College of Engineering, University of Michigan, Ann Arbor, MI 48109 USA.

A. Badano is with the Division of Imaging and Applied Mathematics, Office of Science and Engineering Laboratories, Center for Devices and Radiological Health, U.S. Food and Drug Administration, Rockville, MD 20857 USA.

J. Kanicki is with the Solid-State Electronics Laboratory, Department of Electrical Engineering and Computer Science, and the Macromolecular Science and Engineering, University of Michigan, Ann Arbor, MI 48109 USA and also with the Center for Polymers and Organic Solids, University of California, Santa Barbara, CA 93106 USA (e-mail: kanicki@eecs.umich.edu).

Digital Object Identifier 10.1109/JSTQE.2004.824073

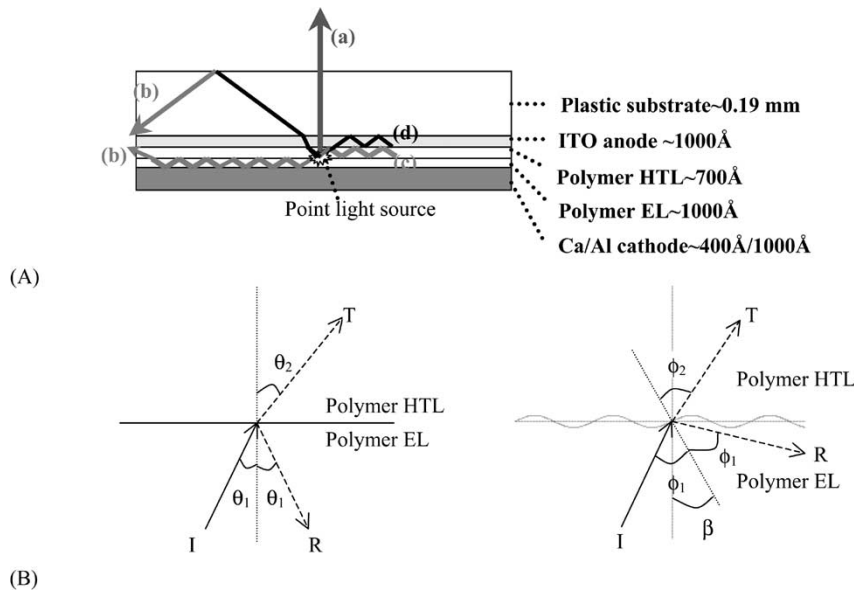


Fig. 1. (A) Schematic representation of the PLED structure used in this paper. A point light source was specified at the interface between the polymer hole transport layer (HTL) and polymer emissive layer (EL). The generated light has four fates: (a) emitted through the front surface; (b) waveguided within the device and exit through device edges; (c) absorbed in the absorptive materials; and (d) trapped by the ITO thin film and eventually got absorbed in the device. (B) Two-dimensional representation of the rough surface model. The rough surface is specified at the interface between polymer EL and polymer HTL. θ_1 and θ_2 are given by Snell's law. On the left, the flat surface case is depicted. The surface normal is rotated within an angle β on the right. After the boundary analysis is performed in the rotated system, T or R are expressed in the original coordinate system.

and transmission coefficients are then interpreted as probabilities. The simulation outcome is calculated by a statistical average of the fate of all histories according to the desired quantity to be evaluated for each experiment. For the angular distribution of the photon emission, the code tracks the number of output photons detected at various angles exited through the front of the PLEDs. The output photons emitted at various angles are then normalized with respect to photons at the surface normal, thus obtaining the angular distribution function of the light-emission.

In our simulation, we introduce out-coupling efficiency (η_{coup}) to represent the probability that a photon generated at the luminescent center within the PLED, emerges through the front surface of the device, thereby contributing to electroluminescence. The η_{coup} depends strongly on the device structure and on the optical constants of the materials and surface properties, and is always less than unity due to light absorption, edge emission, and light trapping. We can summarize the relevant physical processes that occur as

$$\eta_{\text{coup}} = 1 - \eta_{\text{wav}} - \eta_{\text{abs}} - \eta_t$$

where η_{wav} is the fraction of photons that are wave-guided within the device structure and exited through the device edge (contribution from all layers except ITO thin film is included in this term), η_{abs} is the bulk absorbed fractions within device absorptive layers (contribution from all layers except for photons that are trapped by the ITO thin film and eventually got absorbed in the device is included in this term), and η_t is the fraction of photons that are trapped by the ITO thin film due to the total internal reflection at the ITO/subsequent layer interface and eventually got absorbed in the device. In this simulation, we have neglected the light leakage through the cathode side, and the PL quenching due to polymer compo-

sition variations and the presence of carrier flow within the PLEDs. Electric-field-induced photoluminescence quenching in conjugated polymers has experimentally been confirmed, but cannot be implemented easily in this calculation [18].

To describe Fresnel interactions at uneven surfaces of the type found in light-emissive displays, an algorithm that randomly perturbs the surface normal was developed. The departure from a smooth surface is specified by defining a maximum cone within which surface normal tilting can occur. The tilting angle β , Fig. 1(B), is sampled uniformly from a cosine distribution within the allowed range β_M . The tilting angle used in this simulation represents a surface slope that can be related to nonsmooth surface. We are interested in understanding the change of the out-coupling efficiency for surfaces having undulating profiles. In the method used, a Fresnel analysis is then performed using angles and ϕ_1 and ϕ_2 . The Fresnel equations are solved with the incident photon vector expressed in a rotated coordinate system. The out-coming vector is then rotated back to the initial coordinate system. Additionally, a check-point is performed: $\phi_1 + \beta < \pi/2$, which prevents a reflection to be directed back into the surface. For a reflection occurring in a valley of the surface, the reflected photon may strike a neighboring hill. This is not accounted in the model and, therefore, surface normal distributions should be limited to modest cone angles ($\beta_M < 30^\circ$). This description is appropriate for surfaces having undulating profiles with low aspect ratio. This algorithm is a first approximation to the problem of uneven surfaces found in actual devices, and it is used only to investigate general trends in the simulation data.

B. Experiment

1) *Device Structure:* The organic PLED structure used in this paper is shown in Fig. 1(A). The PLEDs were fabricated on

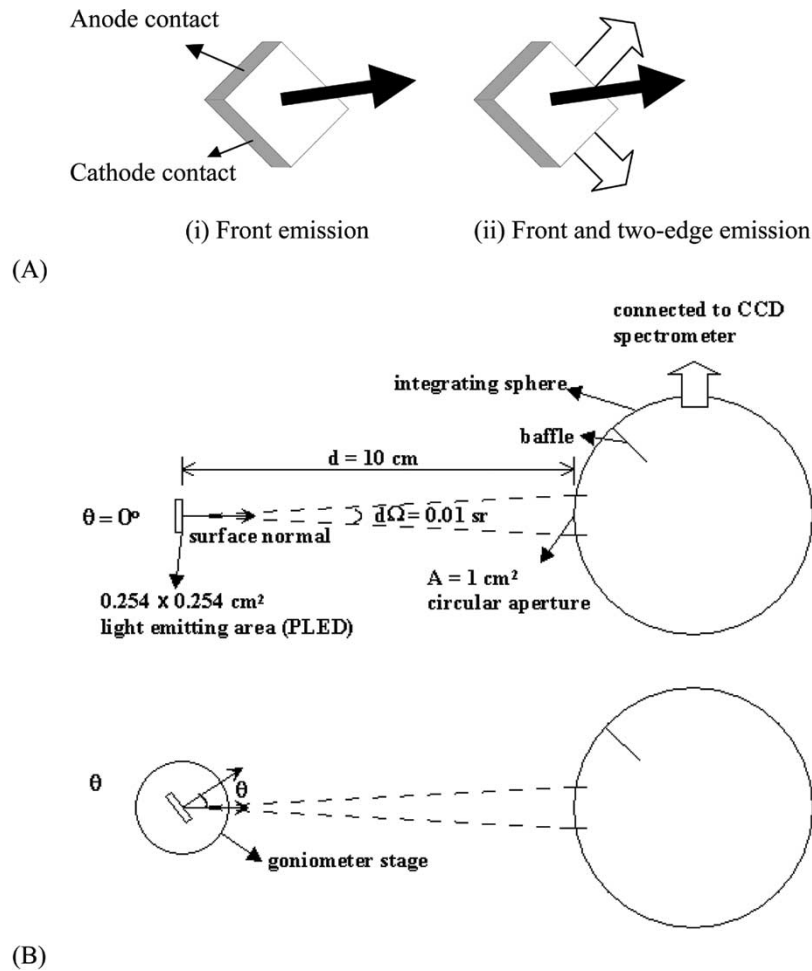


Fig. 2. (A) Schematic representation of the PLED cross sections used for the measurement of the device front and edge light-emissions. (i) Front light emission. (ii) Front and two-edge light emission. (B) Schematic representation of the setup used for the device light-emission angular distribution measurement. The Commission Internationale de l'Éclairage (CIE) standard condition B for the measurement of the averaged LED intensity was used for measuring the PLED light intensity.

the $5 \text{ cm} \times 5 \text{ cm}$ plastic substrates coated with eight patterned ITO fingers. The ITO fingers used as transparent anodes in PLEDs have a sheet resistance of $\sim 10 \text{ ohm}/\square$ and a transparency higher than 80% over the visible range (400–800 nm). The properties of this plastic substrate are described elsewhere [19]. The ITO-covered substrates were cleaned in an ultrasonic bath of isopropanol for 20 min and exposed to UV-ozone for 10 min before polymer spin coating. Next, a hole-transporting layer (HTL, $\sim 700 \text{ \AA}$), poly(3,4-ethylenedioxythiophene)-poly(styrene sulfonate) (PEDOT-PSS), was spin-coated from solution and followed by thermal curing at $90 \text{ }^\circ\text{C}$ for 20 min. Then, light-emissive layer (EL, $\sim 1000 \text{ \AA}$) was spin-coated from solution in xylene and was followed by thermal curing at $90 \text{ }^\circ\text{C}$ for 1 h. The chemical structures of the light-emissive layers are described in [20]. A calcium cathode ($\sim 400 \text{ \AA}$) and an aluminum capping layer ($\sim 2000 \text{ \AA}$) were evaporated through shadow masks in a thermal evaporation system under a high vacuum ($\sim 10^{-7}$ torr). The device area of PLEDs is $0.254 \times 0.254 \text{ cm}^2$ or $0.508 \times 0.508 \text{ cm}^2$.

2) Measurement of the PLED Optoelectronic Properties: The PLEDs front out-coupling and edge wave-guiding light-emissions were measured using an integrating sphere that was calibrated to measure the device total optical flux [15].

In this specific experiment, the PLEDs were placed inside the integrating sphere. When the PLEDs front light-emission measurements were done, we masked all sides of the PLEDs (anode contact, cathode contact, and two remaining edges) with a black mask, and collected only the PLEDs luminous flux from the front as a function of current density, Fig. 2(A). When we measured the PLEDs front + two-edge light-emission, we only masked the anode and cathode contacts with a black mask, and then collected the light emitted from the PLED front and two other edges as a function of current density, Fig. 2(A). We were able to calculate the PLEDs total light-emission (front + 4-edge) value and PLED percent front emission (front emission divided by total emission) by a comparison of the above two measurements and by assuming that the optical flux is the same for each edge.

The absolute PL quantum efficiency measurements of the red and green polymers were performed using the integrating sphere method described in [21] and [22]. It should be noticed that the PL values depend on the solvent used in the film preparation and film air exposure during the measurements. Since the organic polymers can be photo-oxidized under illumination, the polymer PL values are illumination time dependent. The same organic solvent was used for films preparation

needed for PL and EL measurements. However, all PL and EL measurements were done in air at room temperature. Larger PL values are expected when measurements are done under nitrogen atmosphere.

The schematic representation of the setup used for measurements of the PLEDs light-emission angular distribution is shown in Fig. 2(B). In these measurements, we measured only the light-emission from the front with device sides being masked. The device was mounted on a goniometer stage with an angular precision of $\pm 1^\circ$. The detector used for recording the PLEDs light-emission was a CCD spectrometer with an integrating sphere at the front exit. The detector was calibrated with a tungsten filament lamp standard with known spectral irradiance ($\text{W}/\text{cm}^2/\text{nm}$), so the spectral radiant intensity ($\text{W}/\text{sr}/\text{nm}$) of the PLEDs could be accurately measured at the given angle [14]. We adopted the measurement geometry of Commission Internationale de l'Éclairage (CIE) standard condition B for measuring the “averaged LED intensity” at different angles [23]. The CIE standard condition B states that the LED should be positioned facing the detector and aligned so that the mechanical axis of the LED passes through the center of the detector aperture, Fig. 2(B). This condition also involves the use of a detector with a circular entrance aperture having an area (A) of 1 cm^2 and specifies the distance (d) from LED to detector as 10 cm , resulting in the measuring solid angle $d\Omega$ of 0.01 as indicated by the following equation:

$$d\Omega = \frac{A}{d^2}.$$

The PLED spectral radiant intensity was then collected as a function of the external viewing angle (θ) as shown in Fig. 2(B). We then integrated the spectral radiant intensity over the whole spectra region at each angle and normalized the integrated radiant intensity with respect to its value at the angle normal ($\theta = 0^\circ$) to the plane of the PLED. The normalized photon density values at different angles are reported in curve (d) of Fig. 7.

III. RESULTS AND DISCUSSIONS

A. Device Efficiencies

1) *Optical Out-Coupling Efficiency:* The variation of the refractive indices and absorption coefficients with the photon wavelength of the red and green light-emitting polymers used in the simulation was published in [24]. The refractive indices of hole transporting layer were measured by spectroscopic ellipsometry, and the refractive indices of ITO thin film were obtained from the literature [25]. The refractive index of the 0.19-mm -thick transparent plastic substrate was 1.5 . In this analysis, we used the photoluminescent spectra of the green and red light-emitting polymers as the input light source spectra within PLEDs [24]. The input light photons go through refraction, reflection, and absorption events within device structure until they finally exit out of the structures.

In Fig. 3, we show the variation in the calculated values of photon out-coupling (η_{coup}), wave-guiding (η_{wav}), absorption (η_{abs}), and trapping (η_t) components for devices size ranging from $10^{-3} \times 10^{-3} \text{ cm}^2$ to $10^1 \times 10^1 \text{ cm}^2$ for

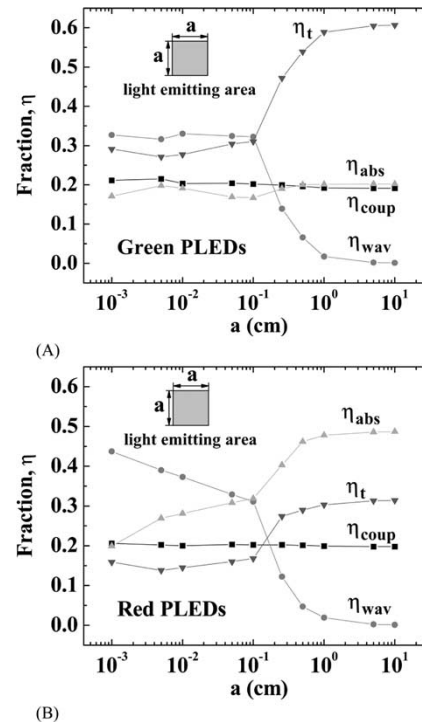


Fig. 3. Photon out-coupling (■), waveguiding (●), absorption (▲), and trapping (▼) fractions of the green (A) and red (B) PLEDs as a function of the device size.

the green and red PLEDs. The Monte Carlo estimates of photon out-coupling (η_{coup}), wave-guiding (η_{wav}), absorption (η_{abs}), and trapping (η_t) values are 0.20 , 0.15 , 0.19 , and 0.46 for $0.254 \times 0.254 \text{ cm}^2$ green PLED and 0.20 , 0.11 , 0.42 , and 0.27 for $0.254 \times 0.254 \text{ cm}^2$ red PLED, respectively. We have observed that the photon out-coupling efficiency is not affected by the wavelength distribution of the photon source for the green and red light-emitting polymers used in this simulation. However, the absorption in polymer layers ($\eta_{\text{abs}} = 0.42$) of red PLED is larger than that of green PLED ($\eta_{\text{abs}} = 0.19$), and trapping/wave-guiding parts in ITO layer ($\eta_t/\eta_{\text{wav}} = 0.27/0.11$) of red PLED are smaller than those of green PLED ($\eta_t/\eta_{\text{wav}} = 0.46/0.15$). Also, for different device sizes the out-coupling efficiencies for both green and red PLEDs are approximately the same and do not change significantly, while the wave-guiding part decreases significantly from ~ 30 to $\sim 0\%$ when PLED sizes increase from $10^{-1} \times 10^{-1} \text{ cm}^2$ to $10^1 \times 10^1 \text{ cm}^2$. The decrease in wave-guiding is due to the increase of absorption in the polymer layers and trapped photons by the ITO thin film when the PLED size increases. Since the refractive indices at 633 nm for the ITO, plastic substrate, and air are ~ 1.8 , ~ 1.5 , and ~ 1 , respectively, the photons reflected from the substrate-air interfaces will enter the ITO layer freely. Therefore, for large PLED sizes, increasing the path of photons will: 1) decrease probability of wave-guiding in plastic substrate; 2) increase probability of absorption in the polymer layer; and 3) increase probability of trapping by the ITO thin-film layer. The quantitative enhancement in the probability of absorption and trapping will depend on the material properties, such as refractive index and absorption coefficients, of each layer.

TABLE I
EXPERIMENTAL PERCENT FRONT EMISSION AND THEORETICAL PERCENT FRONT EMISSION FOR $0.254 \times 0.254 \text{ cm}^2$ AND $0.508 \times 0.508 \text{ cm}^2$ GREEN PLEDs AND $0.254 \times 0.254 \text{ cm}^2$ RED PLEDs ON PLASTIC SUBSTRATE

Sample	Green 0.254×0.254 cm^2	Green 0.508×0.508 cm^2	Red 0.254×0.254 cm^2
Theoretical values without substrate absorption ($\alpha_s = 0 \text{ cm}^{-1}$)			
η_{coup}	19.8 %	19.6 %	20.2 %
η_{wav}	15.3 %	6.57 %	11.0 %
Percent front emission (%)	56.4 %	74.9 %	64.7 %
$\left(\frac{\eta_{\text{coup}}}{\eta_{\text{coup}} + \eta_{\text{wav}}} = \frac{\text{front}}{\text{front} + \text{edge}} \right)$			
Theoretical values with substrate absorption ($\alpha_s = 5.6 \text{ cm}^{-1}$)			
η_{coup}	17.2 %	16.9 %	17.4 %
η_{wav}	7.23 %	1.58 %	5.37 %
Percent front emission (%)	70.4 %	91.5 %	76.4 %
Experimental values			
Front emission efficiency (cd/A)	6.65±0.06	6.29±0.06	0.550±0.01
Edge emission efficiency (cd/A)	1.85±0.06	0.42±0.06	0.145±0.01
Percent front emission (%)	~78 %	~94 %	~79 %

Direct comparison between the theoretical and experimental out-coupling efficiencies is not possible unless the charge injection and charge transport efficiency (η_{charge}), the formation efficiency of the radiative excited electron hole pairs (χ), and photoluminescent efficiency (η_{PL}) are accurately known. Therefore, to validate our simulation results we have compared the Monte Carlo estimates of the η_{coup} and η_{wav} values with the experimental PLEDs front and edge light-emission values for $0.254 \times 0.254 \text{ cm}^2$ and $0.508 \times 0.508 \text{ cm}^2$ green PLEDs and $0.254 \times 0.254 \text{ cm}^2$ red PLEDs. The device configuration is shown in Fig. 1, and calculated and experimental data are given in Table I. We can conclude from this data that there is a discrepancy between the simulated and experimental results if the absorption of the substrate is not taken into considerations. We have further measured the absorption of the plastic substrate by UV-visible absorption spectroscopy, and we obtained that the multilayer plastic substrate has a small absorption coefficient (α_s) of $5.6 \pm 1.0 \text{ cm}^{-1}$ in the visible wavelength region (380–780 nm). By taking the absorption of plastic substrate into consideration, we found a better agreement between the experimental and theoretical results, Table I. We have also shown both experimentally and theoretically that the percent front emission increases with the increasing device size for PLEDs larger than $0.254 \times 0.254 \text{ cm}^2$. The experimental percent front emission is $\sim 78\%$ and $\sim 79\%$ for $0.254 \times 0.254 \text{ cm}^2$ green and red PLEDs, respectively, which

agrees qualitatively with the estimated trend predicted by the Monte Carlo method.

It has been proposed by Tsutsui *et al.* that insertion of a low-index aerogel material ($n_D \sim 1.01 - 1.10$, thickness $\sim 50 \mu\text{m}$) between ITO electrode and glass substrate can enhance the external quantum efficiency by a factor 1.8 because of the decrease in wave-guiding mode in the glass substrate [10]. We have simulated the effect of inserting such a low-index aerogel material ($n_D \sim 1.01 - 1.10$, thickness $\sim 50 \mu\text{m}$) between ITO electrode and plastic substrate into the device structure shown in Fig. 1. We have found that the calculated photon out-coupling (η_{coup}), wave-guiding (η_{wav}), absorption (η_{abs}), and trapping (η_t) fractions are 0.37, 0.09, 0.32, and 0.22 for $0.254 \times 0.254 \text{ cm}^2$ green PLED with the aerogel interlayer. For such devices the out-coupling efficiency is enhanced by a factor of ~ 1.85 in comparison with the PLEDs without the interlayer ($\eta_{\text{coup}} = 0.20$). This simulation is in excellent agreement with Tsutsui *et al.*'s experimental results [10]. Also, our modeling suggested that the increase in the out-coupling efficiency was not due only to the decrease in the wave-guided photons fraction but also to the decrease in the trapped photons by the ITO layer.

We have also investigated the effect of nonsmooth interfaces (as modeled by the algorithm for uneven surfaces described previously in this paper) between the polymer EL and the hole transporting layer on the photon out-coupling, wave-guiding, absorption, and trapping fractions of $0.254 \times 0.254 \text{ cm}^2$ green

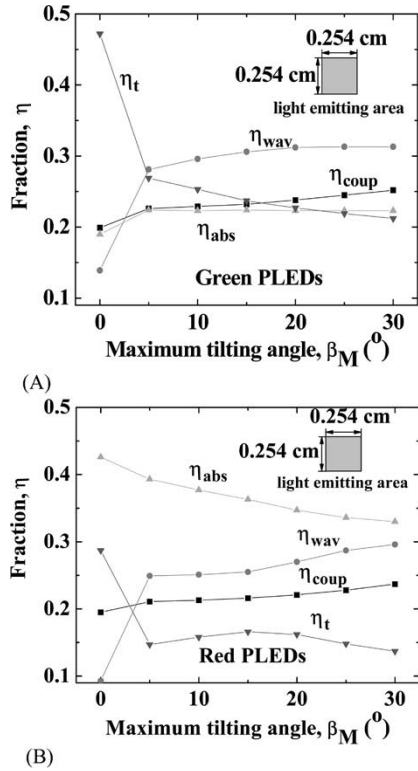


Fig. 4. Photon out-coupling (■), waveguiding (●), absorption (▲), and trapping (▼) fractions of the green (A) and red (B) PLEDs as a function of the maximum surface tilting angle β_M between the polymer emissive and hole transport layers.

and red PLEDs, Fig. 4. Simulated results have shown that sum of the out-coupling and wave-guiding fractions of the generated light of green and red PLEDs increases from 0.34 to 0.57 and from 0.29 to 0.53 when the maximum surface tilting angle β_M increases from 0° to 30° . We have also observed that a non-smooth surface between the polymer emissive and hole transporting layers increases the probability of light transmission within the polymer emissive and hole transporting layers at the expense of the light reflection fraction shown in Fig. 1(B). This profound effect has been observed when the small surface tilting angle ($\beta_M = 5^\circ$) is introduced. These results suggest that randomly roughening the interface of the light-emission region of PLEDs will enhance both the light out-coupling efficiency and wave-guiding efficiency.

2) *External Quantum Efficiency*: The external quantum efficiency (η_{ext}) of the PLEDs is limited by several major losses: the charge injection at the contacts and their transport efficiency within PLED (η_{charge}), the formation efficiency of the radiative excited electron-hole pairs (excitons) (χ), which is also the production efficiency of a singlet exciton, the polymer photoluminescent efficiency (η_{PL}), and the PLED photon out-coupling efficiency (η_{coup}) [3]. Therefore, the (η_{ext}) can be described by

$$\eta_{ext} = \eta_{charge}\chi\eta_{PL}\eta_{coup} = \frac{\# \text{ of emitted photons exiting through the PLED front}}{\# \text{ of electrons flowing through the PLED}}$$

TABLE II
OUT-COUPLING EFFICIENCY (η_{coup}), EXTERNAL QUANTUM EFFICIENCY (η_{ext}), PHOTO-LUMINESCENCE QUANTUM EFFICIENCY (η_{PL}), CHARGE INJECTION AND CHARGE TRANSPORT EFFICIENCY (η_{charge}), AND PRODUCTION EFFICIENCY OF A SINGLET EXCITON (χ) FOR GREEN AND RED PLEDs ON PLASTIC SUBSTRATE

Sample	Green	Red
	$0.254 \times 0.254 \text{ cm}^2$	$0.254 \times 0.254 \text{ cm}^2$
η_{coup}	19.8 %	20.2 %
Maximum η_{ext}	2 %	1.1 %
η_{PL}	$61 \pm 5 \%$	$29 \pm 5 \%$
$\eta_{charge}\chi$	$16.5 \pm 1.4 \%$	$20.0 \pm 3.5 \%$
η_{charge} (assuming $\chi=25\%$)	$66.4 \pm 5.5 \%$	$80.2 \pm 13.8 \%$

the equation at the bottom of this page, where $\#$ of electrons flowing through the PLED = I/q , and

$$\eta_{coup} = \frac{\# \text{ of photons emitted through the PLED front}}{\# \text{ of photons generated within PLED}}$$

The product $\eta_{charge}\chi\eta_{PL}$ defines the intrinsic limitation of the external quantum efficiency of the PLEDs. We define the photon out-coupling efficiency as the ratio of the light output over the internally generated light. We have calculated η_{coup} as $\sim 19.8\%$ and $\sim 20.2\%$ for $0.254 \times 0.254 \text{ cm}^2$ green and red PLEDs, respectively. We also have measured the maximum η_{ext}/η_{PL} as $\sim 2.0\%/ \sim 61 \pm 5\%$ and $\sim 1.1\%/ \sim 29 \pm 5\%$, for green and red PLEDs, respectively, Table II. Therefore, the $\eta_{charge}\chi$ product is estimated to be $\sim 16.5 \pm 1.4\%$ and $\sim 20.0 \pm 3.5\%$ for green and red PLEDs, respectively. If we assume $\chi = 25\%$, we can obtain η_{charge} as $66.4 \pm 5.5\%$ and $80.2 \pm 13.8\%$ for green and red PLEDs, respectively. The charge injection and transport efficiency, η_{charge} , can be enhanced by minimizing the PLED charge injection barrier at the polymer electrode interfaces and better matching between polymer electron and hole mobility values.

B. Angular Distribution

We have investigated the effect of photons refractions, back-reflection from the cathode, absorption by polymer layers, and ITO thin-film effect on the angular distribution of the light-emission from PLEDs. First, we have simulated a simple case where we have considered the effect of refraction between the polymer EL and air and back-reflection from the cathode on photon emission, curve (a) in Fig. 5. Next, we have considered the effect of polymer absorption in addition to the effects mentioned above, curve (b) in Fig. 5. Finally, we have considered the ITO thin-film effect in addition to all effects mentioned above, curve (c) in

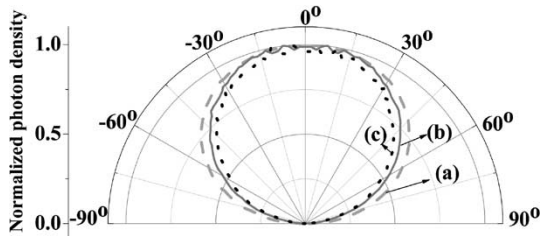


Fig. 5. Simulated angular distribution of the PLEDs front light emission. (a) Simulated result considering the effect of refraction at polymer air interface and back-reflection (--- dash line). (b) Simulated result considering the effect of polymer absorption in addition to refractions and back-reflection (—solid line). (c) Simulated result considering the effect in ITO thin film in addition to refractions, back-reflection, and polymer absorption (... dotted line).

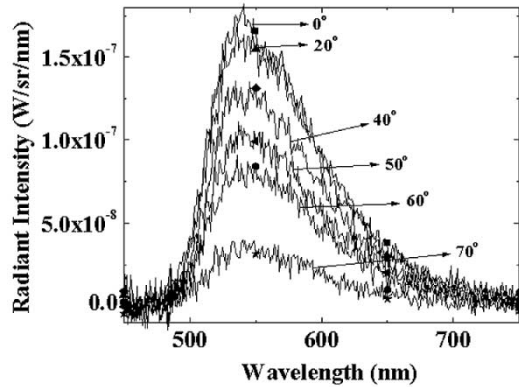


Fig. 6. Measured front electroluminescence spectra of green PLEDs at different angles.

Fig. 7. As can be seen in Fig. 5, the Monte Carlo simulated angular distribution of the PLED light-emission becomes narrower when different effects are added to the simple case. Then, the question is “do we need to consider all these effects in real devices?”

We have measured the electroluminescence spectra of the green PLEDs at different angles, Fig. 6. We can conclude from this figure that the shape of the measured electroluminescence spectra does not change with the measured angle. We then integrated the spectral radiant intensity over the whole spectra region at each angle and we normalized integrated radiant intensity to its value at the normal angle ($\theta = 0^\circ$) to the plane of the PLED. The variation of the normalized photon density for different angles is shown in curve (d) of Fig. 7. The experimental light-emission angular distribution of our green PLED is very close to that of a Lambertian light source, in agreement with the published results [2], [6], [11], [12]. It should be noticed that the light-emission intensity (i.e., flux per solid angle) of a Lambertian surface varies as the cosine of the angle from the normal of the light-emitting surface (i.e., $I(\theta) = I_0 \cos \theta$, where θ is the angle from the surface normal, $I(\theta)$ is the light emission intensity at the angle from the surface normal, and I_0 is the light intensity at the surface normal). Also, we have obtained the best agreement between experimental and Monte Carlo simulated results when we take into account refractions in the PLED, back-reflection from the cathode, absorption in polymer layers, and ITO thin-film effect. Based on these results, we can conclude that all effects must be taken into consideration

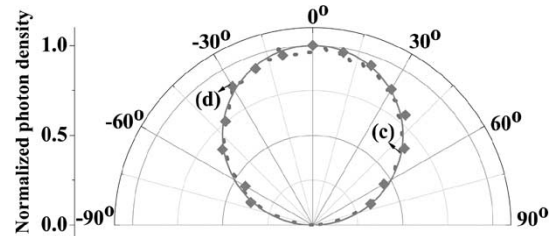


Fig. 7. Experimental and simulated angular distribution of the PLEDs light emission: (c) simulated result considering the effect of back-reflection, refractions, polymer absorption, and ITO thin film (... dot line), and (d) experimental data (diamond). The background gray solid line represents the Lambertian angular distribution of the light source.

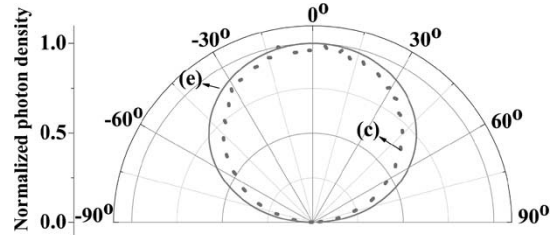


Fig. 8. Angular distribution of the PLEDs light emission: (c) Monte Carlo simulated result considering the effect of back-reflection, refractions, polymer absorption, and ITO thin film (... dot line), and (e) result from a different model proposed by Greenham *et al.* [2] (— solid line).

when we compare simulated and experimental PLED optoelectronic characteristics.

It is important to indicate that our Monte Carlo simulation results are slightly different from Greenham *et al.*'s [2] model result shown in Fig. 8. In their model they assumed that the origin of the Lambertian behavior of polymer light-emitting device is simply due to the refraction at the various interfaces within the device. From our Monte Carlo simulation results, it is obvious that the Lambertian angular distribution behavior of the PLEDs is not only due to photons refraction at different interfaces, but it is also controlled as expected by polymer layers absorption, and ITO thin-film effect. These contribution should be considered when the simulated PLED optoelectronic properties are compared with the experimental data.

IV. CONCLUSION

We have demonstrated that a light transport Monte Carlo code can be used for modeling the realistic geometry of the PLEDs. This method takes into account the absorption in the polymer layers, multiple refractions within the device structure, back-reflection from the cathode, and ITO thin-film effect. We showed that red ($n_D \sim 1.84$ at 633 nm) and green ($n_D \sim 1.7$ at 633 nm) polymer PLEDs have similar simulated photon out-coupling efficiency, which is about 20%. It should be noticed that this efficiency is a function of the device structure. We also showed that the nonsmooth interfaces between the polymer light-emissive and hole transporting layers increases the probability of the photons out-coupling and wave-guiding fractions of the internally generated light. Finally, we demonstrated that the origin of the Lambertian behavior of the PLEDs is not only due to simple refraction at different interfaces, but it is also determined by polymer layers absorption, and ITO thin-film effect.

ACKNOWLEDGMENT

The authors would like to thank Dr. S. Martin, Y. Hong, and A. Johnson for useful discussions.

REFERENCES

- [1] A. Badano and J. Kanicki, "Monte Carlo analysis of the spectral photon emission and extraction efficiency of organic light-emitting devices," *J. Appl. Phys.*, vol. 90, pp. 1827–1830, 2001.
- [2] N. C. Greenham, R. H. Friend, and D. D. C. Bradley, "Angular dependence of the emission from a conjugated polymer light-emitting diode: Implications for efficiency calculations," *Adv. Mater.*, vol. 6, pp. 491–494, 1994.
- [3] N. K. Patel, S. Cinà, and J. H. Burroughes, "High-efficiency organic light-emitting diodes," *IEEE J. Select. Topics Quantum Electron.*, vol. 8, pp. 346–361, Mar.-Apr. 2002.
- [4] I. Schnitzer, E. Yablonovitch, C. Caneau, T. J. Gmitter, and A. Scherer, "30% external quantum efficiency from surface textured, thin-film light-emitting diodes," *Appl. Phys. Lett.*, vol. 63, pp. 2174–2176, 1993.
- [5] B. J. Matterson, J. M. Lupton, A. F. Safonov, M. G. Salt, W. L. Barnes, and I. D. W. Samuel, "Increased efficiency and controlled light output from a microstructured light-emitting diode," *Adv. Mater.*, vol. 13, pp. 123–127, 2001.
- [6] S. Moller and S. R. Forrest, "Improved light out-coupling in organic light emitting diodes employing ordered microlens arrays," *J. Appl. Phys.*, vol. 91, pp. 3324–3327, 2002.
- [7] T. Yamasaki, K. Sumioka, and T. Tsutsui, "Organic light-emitting device with an ordered monolayer of silica microspheres as a scattering medium," *Appl. Phys. Lett.*, vol. 76, pp. 1243–1245, 2000.
- [8] I. Schnitzer, E. Yablonovitch, C. Caneau, and T. J. Gmitter, "Ultrahigh spontaneous emission quantum efficiency, 99.7% internally and 72% externally, from AlGaAs/GaAs/AlGaAs double heterostructures," *Appl. Phys. Lett.*, vol. 62, pp. 131–133, 1993.
- [9] R. H. Jordan, L. J. Rothberg, A. Dodabalapur, and R. E. Slusher, "Efficiency enhancement of microcavity organic light emitting diodes," *Appl. Phys. Lett.*, vol. 69, pp. 1997–1999, 1996.
- [10] T. Tsutsui, M. Yahiro, H. Yokogawa, K. Kawano, and M. Yokoyama, "Doubling coupling-out efficiency in organic light emitting devices using a thin silica aerogel layer," *Adv. Mater.*, vol. 13, pp. 1149–1152, 2001.
- [11] J. S. Kim, P. K. H. Ho, N. C. Greenham, and R. H. Friend, "Electroluminescence emission pattern of organic light-emitting diodes: Implications for device efficiency calculations," *J. Appl. Phys.*, vol. 88, pp. 1073–1081, 2000.
- [12] M. H. Lu and J. C. Sturm, "Optimization of external coupling and light emission in organic light-emitting devices: Modeling and experiment," *J. Appl. Phys.*, vol. 91, pp. 595–604, 2002.
- [13] V. Bulović, V. B. Khalfin, G. Gu, P. E. Burrows, D. Z. Garbuzov, and S. R. Forrest, "Weak microcavity effects in organic light-emitting devices," *Phys. Rev. B*, vol. 58, pp. 3730–3740, 1998.
- [14] S. J. Lee, A. Badano, and J. Kanicki, "Monte Carlo simulation and optoelectronic properties of organic light-emitting devices on flexible plastic substrates," in *Proc. Conf. Record 23rd Int. Display REs Conf.*, 2003, pp. 26–29.
- [15] —, "Integrating sphere CCD-based measurement method for organic light-emitting devices," *Rev. Sci. Instrum.*, vol. 74, pp. 3572–3575, 2003, to be published.
- [16] A. Badano, "Optical blur and collection efficiency in columnar phosphors for X-ray imaging," *Nucl. Instrum. Meth. A*, vol. 508, pp. 467–479, 2003.
- [17] —, "Modeling the bidirectional reflectance of emissive displays," *Appl. Opt.*, vol. 42, pp. 3847–3852, 2002.
- [18] S. J. Lee and J. Kanicki, Unpublished Results.
- [19] Y. Hong, Z. He, J. Kanicki, and N. S. Lennhoff, "Flexible plastic substrates for organic light-emitting displays and other devices," *J. Electron. Mater.*, vol. 33, pp. 312–320, 2004.
- [20] M. T. Bernius, M. Inbasekaran, J. O'Brien, and W. Wu, "Progress with light-emitting polymers," *Adv. Mater.*, vol. 12, pp. 1737–1750, 2000.
- [21] J. C. de Mello, H. F. Wittmann, and R. H. Friend, "An improved experimental determination of external photoluminescence quantum efficiency," *Adv. Mater.*, vol. 9, pp. 230–23, 1997.
- [22] S. J. Lee, J. Klein, and J. Kanicki, Unpublished Results.
- [23] Commission Internationale de l'Éclairage, Measurement of LED's, in Publication CIE 127, pp. 12–16, 1997.
- [24] S. J. Lee, A. Badano, and J. Kanicki, "Monte Carlo modeling of organic polymer light-emitting devices on flexible plastic substrates," *Proc. SPIE*, vol. 4800, pp. 156–163, 2003.

- [25] T. Gerfin and M. Grätzel, "Optical properties of tin-doped indium oxide determined by spectroscopic ellipsometry," *J. Appl. Phys.*, vol. 79, pp. 1722–1729, 1996.
- [26] K. A. Neys, "Imulation of light emission from thin-film microcavities," *J. Opt. Soc. Am. A*, vol. 15, pp. 962–971, 1998.



Shu-jeen Lee received the B.S. and M.S. degrees in chemical engineering from the National Taiwan University, Taipei, Taiwan, in 1997 and 1999, respectively. She is working toward the Ph.D. degree in macromolecular science and engineering at the University of Michigan, Ann Arbor, since September 1999.

Since September 2000, she has been with the Organic and Molecular Electronics Group, Electrical Engineering Department, University of Michigan. During her Ph.D. study, she investigated new materials and device structures for PLEDs, designed optical structures to optimize the PLED's performance, integrated the PLEDs with the active-matrix circuitry, and developed advanced characterization methods for evaluating a prototype active matrix, polymer light-emitting display (AM-PLED).



Aldo Badano received the Ph.D. degree in nuclear engineering from the University of Michigan, Ann Arbor, in 1999.

He is currently a Research Scientist with the Division of Imaging and Applied Mathematics, Office of Science and Engineering Laboratories, Center for Devices and Radiological Health, U.S. Food and Drug Administration, Rockville, MD, where he has developed a program on the evaluation of medical displays. His research focuses on the objective assessment of image quality in medical imaging sensors and image display devices using advanced experimental and computational methods. He is a referee for several scientific journals and a reviewer of technical grants for DOD and NIH. He has authored and coauthored more than 50 publications.

Dr. Badano is a Member of SID, AAPM, and The International Society for Optical Engineers (SPIE).



Jerzy Kanicki (M'99–A'99–SM'00) received the Ph.D. degree in sciences (D.Sc.) from the Free University of Brussels (Université Libre de Bruxelles), Brussels, Belgium, in 1982. His dissertation research work involved the "Optical, electrical, and photovoltaic properties of undoped and doped trans-polyacetylene."

He subsequently joined the IBM Thomas J. Watson Research Center, Yorktown Heights, NY, as a Research Staff Member working on hydrogenated amorphous silicon devices for the photovoltaic and flat-panel display applications. In 1994, he moved from IBM Research Division to the University of Michigan, Ann Arbor, as a Professor in the Department of Electrical Engineering and Computer Science (EECS). He is the author and coauthor of over 200 publications in journals and conference proceedings. He has edited two books and three conference proceedings. At present, his research interests within the Electrical and Computer Engineering (ECE) Division of EECS include organic and molecular electronics, thin-film transistors and circuits, and flat-panel displays technology including organic light-emitting devices.

Dr. Kanicki served as Organizing Chairman and/or Co-Chairman of the Amorphous Insulating Thin Films Symposia (Boston, MA, 1992; Strasbourg, France, 1994; Osaka, Japan, 1995) and the 1988 International Conference on Hydrogenated Amorphous Silicon Devices and Technology, Yorktown Heights, NY. He received several IBM External Honors Prizes in 1989, 1990, and 1993. He is a Member of SID, the American Chemical Society (ACS), the American Physical Society (APS), and MRS.